

Interaction of Gadolinium-Based MR Contrast Agents With Choline: Implications for MR Spectroscopy (MRS) of the Breast

Robert E. Lenkinski,* Xiaoen Wang, Mostafa Elian, and S. Nahum Goldberg

It has been shown that magnetic resonance spectroscopy (MRS) can improve the specificity of the MR examination by the spectroscopic detection of choline (Cho). Commonly, the lesion is first visualized on postcontrast studies, and the MRS voxel is prescribed accordingly. The implicit assumption made in this approach is that the presence of gadolinium-based contrast agents will have a negligible effect on the MR spectra obtained from the lesion. In this work, we examined this assumption by determining the effects of six gadolinium-based contrast agents: Magnevist, Multihance, Omniscan, Optimark, ProHance, and Dotarem, on the Cho peak in phantoms and in a rat model for breast cancer. We found that only the three negatively-charged chelates: Magnevist, MultiHance, and Dotarem, broadened the Cho peak in phantoms and reduced the area of the Cho peak in vivo by an average of about 40%. The use of negatively-charged chelates may lead to an underestimation of the levels of Cho present in human breast cancers, since most studies use MRS postcontrast administration. Therefore, we recommend the use of the neutral chelates in MRI/MRS studies of the breast. Magn Reson Med 61:1286–1292, 2009. © 2009 Wiley-Liss, Inc.

Key words: breast MRS; contrast agents; interactions; choline; in vivo

There is increasing adoption of MRI of the breast both as a screening examination for younger women who are at high risk for developing breast cancer (1–3) or as a problem-solving tool following mammography and/or ultrasound imaging (4–8). The visualization and characterization of breast lesions on MRI is based on a combination of morphological features of the lesion precontrast injection and patterns of dynamic contrast enhancement postinjection of gadolinium-based contrast agents. Recently, it has been shown that magnetic resonance spectroscopy (MRS) can improve the specificity of the MR examination by the spectroscopic detection of choline (Cho)-containing compounds (see Refs. 9–13 for reviews). The majority of the in vivo MRS studies were performed using single-voxel methods, where the lesion was first visualized on the postcontrast studies and the MRS voxel prescribed accordingly. The implicit assumption made in this approach is that the presence of gadolinium-based contrast agents will have a negligible effect on the MR spectra obtained from

the lesion. The only report that has addressed this issue explicitly in breast MRS is the study of Joe et al. (14), which showed that there were changes in both the line-width (increase of 15–21%) and area (decrease of 11–18%) of the Cho peak, in the same subjects, pre- and postinjection of Omniscan (gadodiamide). There have been several reports addressing the effects of gadolinium-containing contrast agents on MR spectra both in vitro (15,16) and in vivo (17–22). All of the in vivo studies involved determining the effects of gadolinium diethylenetriamine penta acetate (Gd-DTPA; Magnevist) or gadolinium-tetraazacyclododecane tetra acetate (Gd-DOTA; Dotarem) on the proton MRS of brain tumors. Although the in vitro studies reported significant alterations in the spectral properties of Cho in phantoms, in the presence of Gd-DTPA, the in vivo studies reported smaller changes (10–15%) in the Cho peak postcontrast administration. This smaller change was attributed to the fact that in the brain the Cho is predominantly intracellular and thus cannot come into direct contact with the contrast agent.

There are currently five gadolinium-based contrast agents approved for human use in the United States. These are: Magnevist, Multihance, Omniscan, Optimark, and ProHance (see Fig. 1 for the chemical names). The structures of these five agents and a sixth agent, Dotarem, which was part of the studies of brain MRS reported by Sijens et al. (19–21), are shown in Fig. 1. Note that three of these agents are neutral at physiological pH, i.e., they have no overall charge (Omniscan, Optimark, and ProHance), while the other three agents (Magnevist, Multihance, and Dotarem) are negatively charged. It has been suggested that the charge of the agent is important since Cho is a positively-charged molecule at neutral pH and in solution Cho can form a weak complex with negatively-charged gadolinium chelates (22,23). The situation in vivo may be complicated by the fact that Cho must come into direct contact with the contrast agent in order to form a complex. The formation of this complex can lead to shortening of the relaxation times of the methyl protons of Cho through the electron–nuclear dipole interaction.

The overall goal of this work was to determine the effects of the six gadolinium-containing contrast agents, shown in Fig. 1, on the proton MRS resonance of Cho, both in phantoms and in an animal model for breast cancer. We discuss the implications of these findings with respect to clinical MRS studies of breast lesions.

MATERIALS AND METHODS

All of the MRI/MRS studies were performed on 3.0T GE Signa short-bore twin speed system (GE Healthcare, Mil-

Department of Radiology, Beth Israel Deaconess Medical Center, Harvard Medical School, Boston, Massachusetts, USA.

*Correspondence to: Robert E. Lenkinski, Prof., Department of Radiology Beth Israel Deaconess Medical Center, 330 Brookline Avenue Boston, MA 02215. E-mail: rlenkins@bidmc.harvard.edu

Received 25 July 2008; revised 5 November 2008; accepted 3 December 2008.

DOI 10.1002/mrm.21937

Published online 13 April 2009 in Wiley InterScience (www.interscience.wiley.com).

© 2009 Wiley-Liss, Inc.

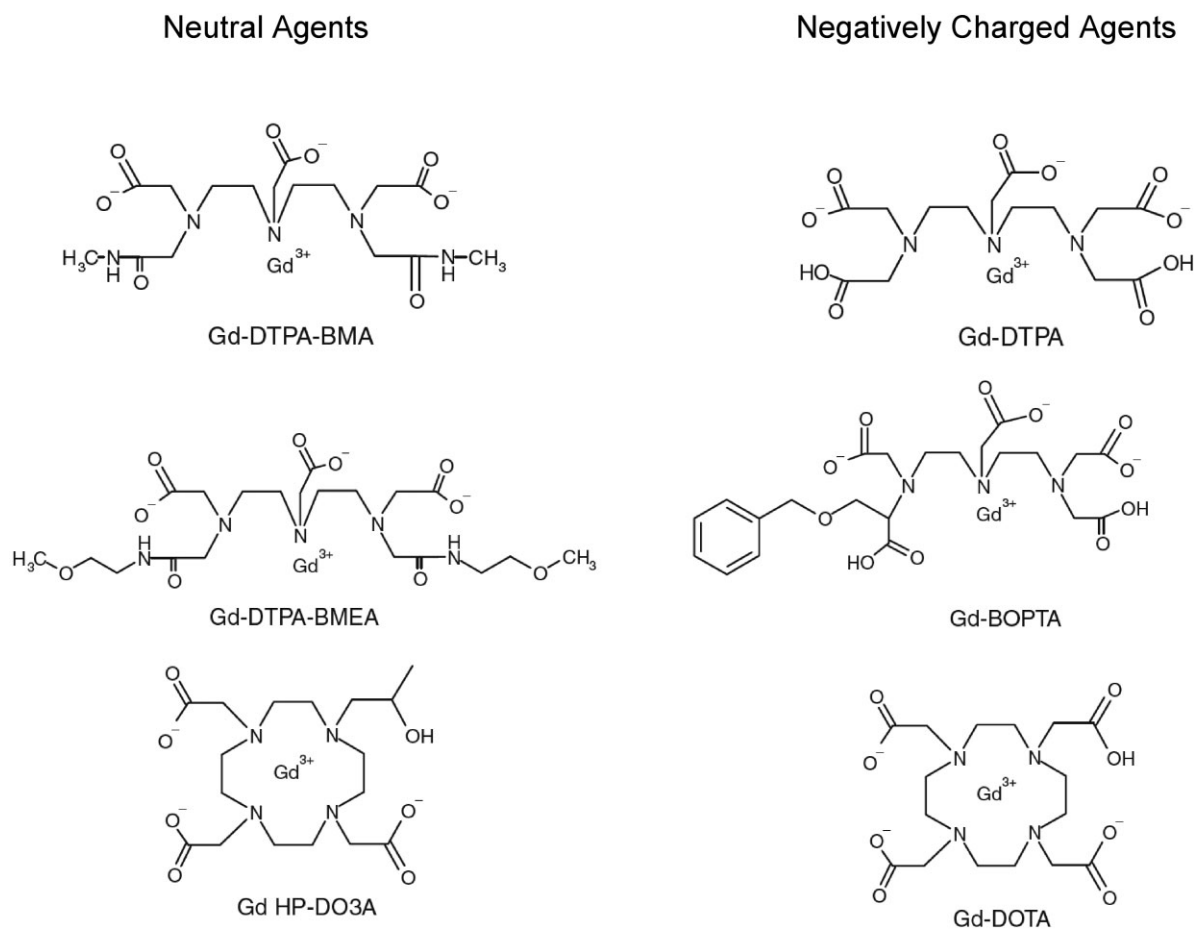


FIG. 1. The chemical structures of the six gadolinium-based contrast agents used in this study. Gd-DTPA-BMA is Omniscan, Gd-DTPA-BMEA is OptiMark, Gd-HP-DO3A is ProHance, Gd-DTPA is Magnevist, Gd-BOPTA is MultiHance, and Gd-DOTA is Dotarem.

waukee, WI, USA). The standard head coil was used for the *in vitro* studies. The animal studies were performed using a custom-built quadrature birdcage coil (diameter = 6 cm, length = 10 cm).

In Vitro Studies

We prepared a 250-ml solution containing 10 mM Cho (choline chloride; Aldrich, St. Louis, MO, USA) at pH 7.2. Single-voxel MR spectra were acquired sequentially using the point-resolved spectroscopy sequence (PRESS) method from a $1 \times 1 \times 1$ cm³ voxel with a TR = 2 s and a TE = 144 msec, before and after serial additions of a solution containing 10 mM Cho and 250 mM of each of the six contrast agents. The T_2 of Cho was estimated from the line-width of the Cho peak. We also measured the T_1 of the Cho peak in each case using a progressive saturation method. These studies were repeated at a 15 mM Cho concentration after sequential additions of a solution containing 15 mM Cho and 250 mM of each of the six agents.

In Vivo Studies

All of the animal experiments were performed with the approval of our institutional committee for animal research and in accordance with the guidelines of the Na-

tional Institutes of Health for the care and use of laboratory animals. For all of the experiments and procedures, anesthesia was induced by means of an intraperitoneal injection of a mixture of ketamine (Phoenix Pharmaceutical, St. Joseph, MO, USA), at a dose of 75 mg/kg of body weight, and xylazine (Bayer, Shawnee Mission, KA, USA), at a dose of 10 mg/kg. A total of 24 six-week-old female Fischer-344 rats (Taconic Farms, Germantown, NY, USA) were injected with 0.2–0.3 ml of R3230 mammary adenocarcinoma cell suspension (1×10^8 cells/ml) into the hind limb (see Ref. 24 for details about the tumor model). These studies were performed when the desired tumor size (1.5–3.0 cm) was achieved. Rats were anesthetized before each MR examination; a 24-gauge catheter was inserted into the tail vein for injection of the contrast agent during the MR examination.

Rats were placed in the prone position; the tumors were set at the center of the birdcage coil. Following the three-plane localization sequence, each animal was imaged using a T_1 -weighted spin-echo sequence (TR = 300 ms, TE = 11 ms, slice thickness = 3.0 mm, matrix size = 256×128 , FOV = 8×8 cm², number of excitations [NEX] = 2). Localized ¹H-MRS was acquired from a $1 \times 1 \times 1$ cm³ voxel centered in the tumor using the PRESS method with water suppression (TR = 2 s; TE = 144 ms, data points =

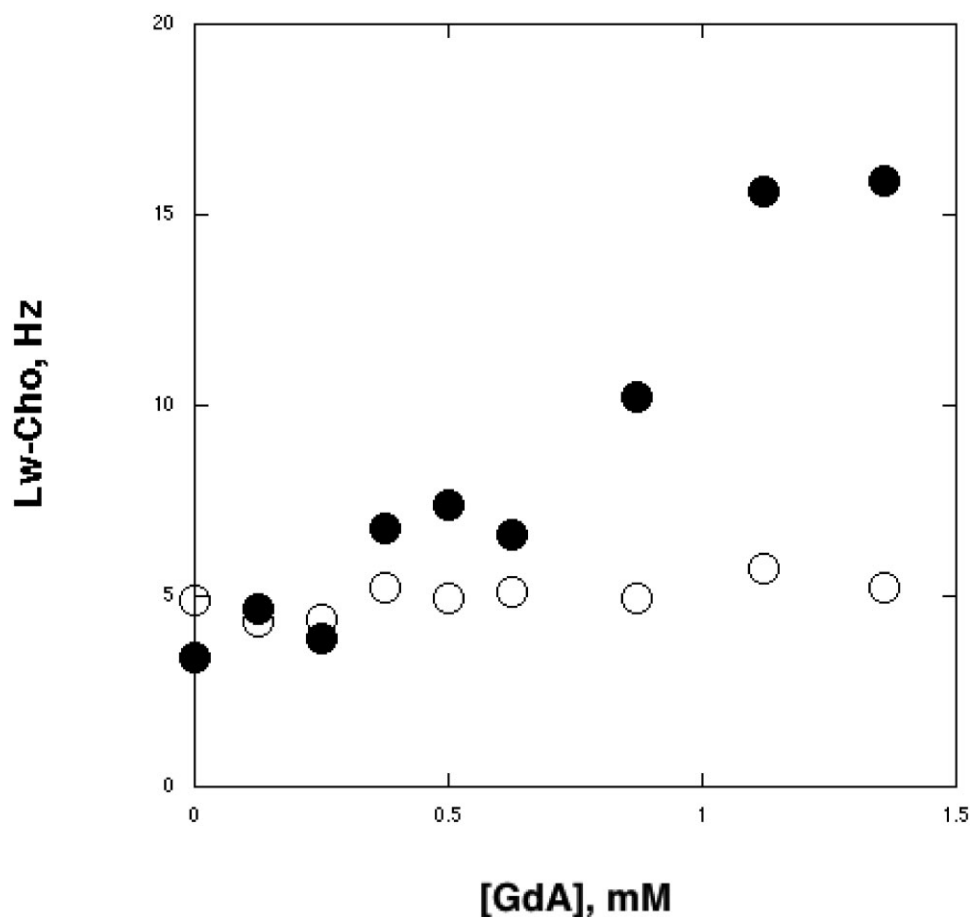


FIG. 2. The variation in the line-width of choline (10 mM) as a function of added contrast agent. The filled circles indicate Magnevist, and the open circles are for Omniscan.

2048, sweepwidth = 2500 Hz, and averages = 256). Following the automated shimming, the homogeneity was checked manually and adjusted, if necessary, for each acquisition. In order to examine the reproducibility of the ^1H MR spectroscopy, the spectroscopy was performed twice in six rats before the administration of the contrast agents.

For each of the six contrast agents, data were acquired in four rats prior to and after the tail vein injection of 0.1 mM/kg of each agent. The T_1 -weighted spin-echo sequence (TR = 300 ms, TE = 11 ms, slice thickness = 3.0 mm, matrix size = 256×128 , FOV = 8×8 cm 2 , NEX = 2) was repeated postinjection for 15 min. The voxel location and voxel size for postcontrast spectroscopy was copied from the precontrast spectroscopy sequence, and the postcontrast MRS acquisition was started approximately 15 min postinjection.

Data Analysis

Spectra were processed using SAGE spectral analysis software (General Electric Healthcare Technologies, Milwaukee, WI, USA). Processing included 120-Hz high-pass filter, Gaussian apodization, Fourier transformation, phase, frequency, and baseline corrections. The area and the line-width of the Cho peak was determined with the automatic curve fitting routine operating in the frequency domain.

To examine the reproducibility of the ^1H MRS we used in this study, we analyzed the Cho peak area differences in

two acquisitions in six rats before the administration of contrast agent using the correlation coefficient and the Bland-Altman method (25). A statistical comparison of pre- and postcontrast measurements was performed using a paired t -test. A P -value < 0.05 was considered statistically significant.

RESULTS

In Vitro Studies

Examples of the increases in the line-width of the Cho resonance with increasing agent concentrations are shown in Fig. 2 for the 10-mM Cho experiment. All three of the negatively-charged chelates (Magnevist, Multihance, and Dotarem) broadened the Cho resonance in an almost identical manner. These three agents also shortened the T_1 of the Cho resonance in a similar manner. The neutral chelates (Omniscan, Optimark, and ProHance) had little or no effect on either the T_1 or line-width of the Cho peak. If we assume that the negatively-charged chelates form a 1:1 complex with Cho, then the dissociation constant, KD, is defined as

$$K^D = \frac{[\text{GdA}][\text{Cho}]}{[\text{GdA-Cho}]} \quad [1]$$

where GdA refers to the Gd contrast agent, Cho refers to choline, GdA-Cho refers to the complex, and [] denote

equilibrium concentration. The transverse relaxation rate ($\pi \Delta\omega 1/2$) at each GdA concentration, $1/T_{2obs}$, is given by

$$1/T_{2obs} = 1/T_{20} + Pm/Tm \quad [2]$$

where $1/T_{20}$ is the transverse relaxation rate before the addition of contrast agent, $P_M = [GdA - Cho]/Cho_T$ (Cho_T is the formal concentration of Cho) and $1/T_{2M}$ is the transverse relaxation rate in the GdA - Cho complex. Mass balance requires that

$$GdA_T = [GdA] + [GdA - Cho] \quad [3]$$

and

$$Cho_T = [Cho] + [GdA - Cho] \quad [4]$$

be true.

Since the concentration of Cho, Cho_T , is much larger than GdA_T , we can assume that $[Cho]$ is approximately equal to Cho_T . Rearranging Eq. [1] using this assumption with mass balance, and substituting into Eq. [2] gives the following:

$$1/T_{2obs} = 1/T_{20} + \frac{(GdA_T)}{(K_D + Cho_T)T_{2M}} \quad [5]$$

Thus a plot of $1/T_{2obs}$ vs. the concentration of the agent added should be linear with a slope of $1/(K_D + Cho_T)T_{2M}$. An identical relationship can be derived for $1/T_{1obs}$. Repeating this experiment at two different Cho concentrations can lead to the determination of both K_D and $1/T_{2M}$ from the two values of the slopes of these plots. We found that all of the plots constructed based on either Eq. [5] or the same relationship for $1/T_{1obs}$ were linear (see Fig. 2 for an example). From linear regression analysis we determined that the slopes of the lines found for the line-widths of 10 mM and 15 mM Cho experiments carried out with Magnevist were 9.9 and 7.5, respectively. From these slopes we derived values for K_D of around 0.05 M^{-1} (range = $0.045\text{--}0.06 \text{ M}^{-1}$) for Magnevist, MultiHance, and Dotarem, with no significant difference between the individual results. The corresponding values for $1/T_{2M}$ were around 1400 s^{-1} (range = $1300\text{--}1500 \text{ s}^{-1}$). Similar values were found for the analysis of the T_1 results with an average value for T_{1M} of about 0.7 ms.

The well-known Solomon equation (26–29) describes the relationship between $1/T_{2M}$, $1/T_{1M}$, and r , the distance between the paramagnetic center and the protons being relaxed

$$1/T_{2M} = Dr^{-6}f(\tau_c) \quad [6]$$

where D is a known constant and $f(\tau_c)$ is a function of correlation times. The relevant value for τ_c in Eq. [6] is the rotation correlation time for the complexes, which has been reported to be around $55 \times 10^{-12} \text{ s}$ for Magnevist, MultiHance, and Dotarem (30). Using this value and 1400 s^{-1} for $1/T_{2M}$ gives an average value for r of about 8.2 \AA , which is in good agreement with the distance reported by Elgavish and Reuben (23) for the complexes of tri-methyl-

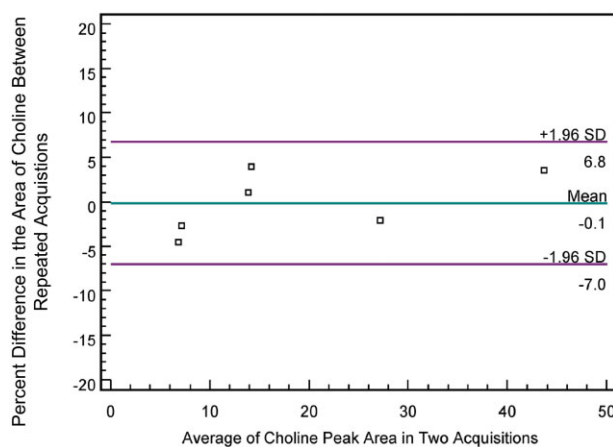


FIG. 3. Bland-Altman plots constructed from repeated choline peak area measurement in two acquisitions performed precontrast.

ammonium ions and Gd(ethylene diamine tetra acetate [EDTA]).

Reproducibility of In Vivo MRS

We analyzed the results of the repeated MRS acquisitions that were performed precontrast. The correlation coefficient was highly statistically significant ($r = 0.99$, $P < 0.001$) for repeated analysis of the area of the Cho peak from the pairs of repeated spectra. The results of Bland-Altman analysis for these repeat MRS acquisitions are shown in Fig. 3. There is very good agreement between the area of the Cho peak measurement in the two acquisitions. We found that even though there is some variability in the area of the Cho peak across different tumors, the mean difference between repeated measurements on the same tumor is less than 1% and the limits of agreement (1.96 times the standard deviation) are -7.1% and 6.8% respectively.

IN VIVO STUDIES

All of the tumors exhibited significant enhancement on the postcontrast MRI and a clear Cho peak (3.2 ppm) on the $^1\text{H-MR}$ spectra obtained both precontrast and postcontrast. Examples of studies carried out with Magnevist (negatively charged) and Omniscan (neutral) are shown in Fig. 4. The administration of Magnevist decreased the area of the Cho peak by 47.3% in the spectrum (Fig. 4a), whereas there was a small, but not statistically significant, decrease in the area of the Cho peak (6.2%) in the spectrum acquired post-Omniscan (neutral chelate) administration (Fig. 4b). Note that in Fig. 4, even though the peak area of Cho has decreased, there is little or no line-broadening observed in the residual Cho peak acquired postcontrast. In the postcontrast spectrum obtained with Omniscan, there is also no change observed in the line-width of the Cho resonance. All of the negatively-charged agents showed behavior similar to that shown for Magnevist, while none of the neutral chelates had any appreciable effect on the Cho peak (see Fig. 5a). The decrease in the area of the Cho peak postcontrast for each of the three negatively-

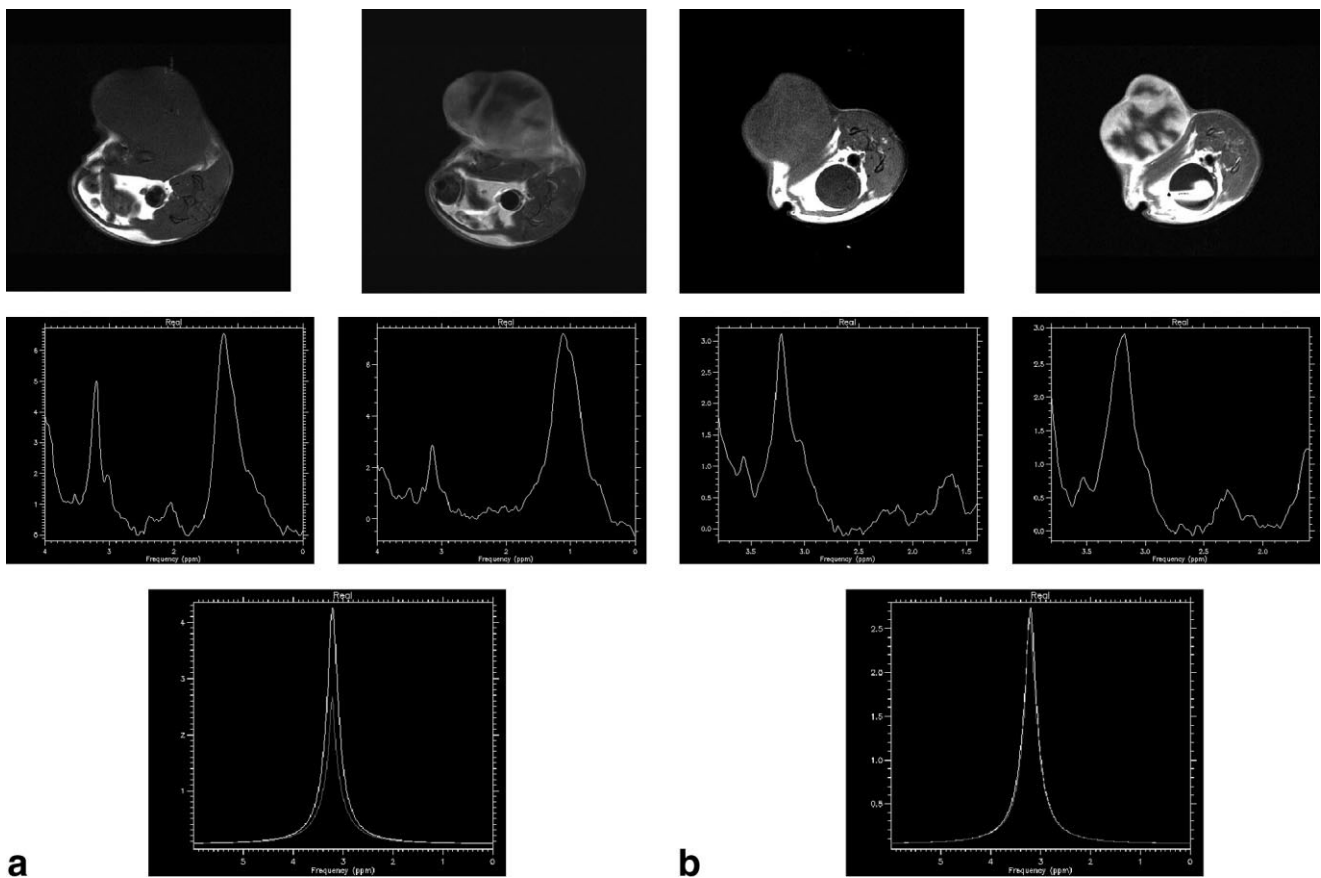


FIG. 4. The representative MR spectra (middle row) prior to (middle left in (a) and (b)) and 15 min after injection of Magnevist (middle right in (a)) and Omniscan (middle right in (b)). The fitted overlay spectra (bottom row) show the relative choline peak decrease in the postcontrast spectra (red) of Magnevist (bottom left) and Omniscan (bottom right). The pre- and post-MR images are shown above.

charged chelates and the three neutral chelates is shown in Fig. 5. These decreases were found to be statistically significant ($P < 0.001$). Figure 5b shows the decrease in the area of the Cho peak area averaged across the group of negatively-charged chelates and the group of neutral

chelates. The average decrease in the Cho peak area in the postcontrast spectra was $42.8\% \pm 17.1\%$ (range = 21.8–76.1%) for the negatively charged chelates, whereas for the neutral chelates this decrease was $5.0\% \pm 4.9\%$ (range = 0–11.2%).

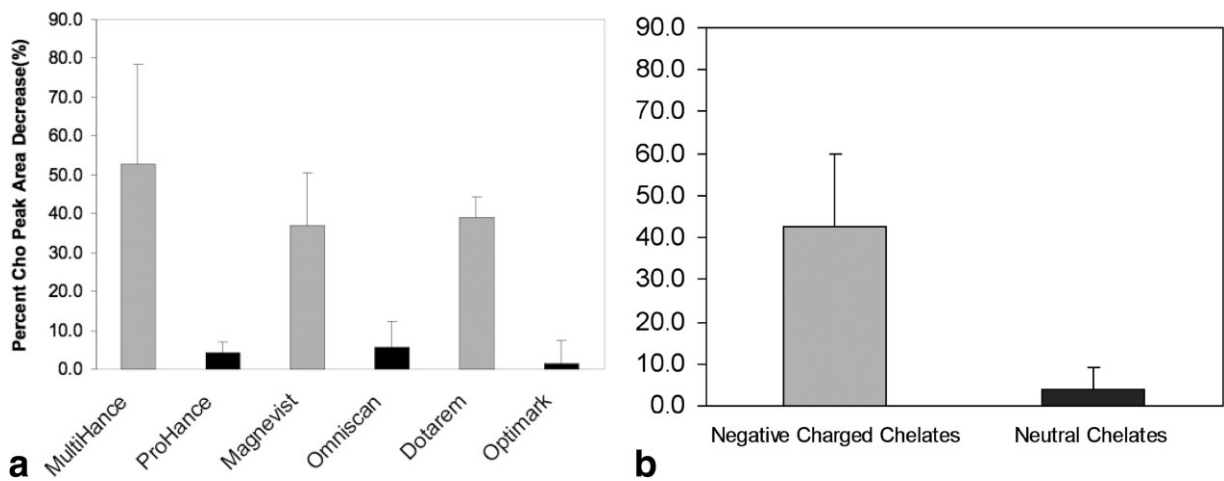


FIG. 5. **a:** The comparison of choline peak area decrease on postcontrast spectra for the three negatively-charged chelates (gray bar) and the three neutral chelates (black bar) for the individual contrast agents. **b:** The comparison of the decrease in the area of the choline peak averaged across the negative chelates and neutral chelates. The differences are statistically significant ($P < 0.001$).

DISCUSSION

We have shown that in aqueous solution, of the six agents studied, only the three negatively-charged gadolinium-based chelates form ion pairs with Cho. The agreement between the effects observed on both the T_1 and line-width of the Cho resonance in vitro clearly demonstrate that the electron–nuclear dipolar interaction dominates (Eq. [6]), and there is a direct interaction between Cho and these three paramagnetic agents. For these negatively-charged agents, the dissociation constants and limiting relaxation properties are quite similar to each other and to Gd(EDTA) (23), suggesting that the structures of the ion pairs are also quite similar. The common feature of these three chelates is the presence of a free carboxylate group even though two of the agents are linear chelates, Magnevist and MultiHance, and the other, Dotarem, is a macrocyclic chelate. The distance between the methyl groups on the Cho and the Gd, derived from an analysis of the limiting line-width or T_1 , is approximately 10 Å, which is consistent with the binding of the Cho head group to the free carboxylate (23). This distance may be approximate since the Cho methyls rotate freely in space and thus are weighted by the $1/(r^6)$ function (31). The three neutral chelates showed negligible effects on the Cho resonance in solution. To our knowledge, our study is the first to show the importance of the charge of the chelate on its binding to Cho, although this point has been made in studies of the effects of individual agents on the Cho resonance (22).

The situation found in vivo is consistent with the observations made in vitro. That is, the three negatively-charged chelates decreased the area of the Cho peak by about 40%, while the neutral chelates had little or no effect. This decrease is about four times larger than the variability we found for the in vivo MRS results. The fact that the line-width of the residual Cho resonance in the presence of the negatively-charged chelates showed minimal line-broadening and that the three neutral chelates had only small effects on the line-width of the Cho peak without affecting its area indicates that these observations can only be explained by direct interactions of Cho with the contrast agents rather than through any bulk susceptibility effects. The most straightforward explanation from an MR point of view is that the gadolinium agents distribute through the extracellular space in tumors and there must be direct contact (ion-pair formation) in order to broaden 40% of the Cho pool to past the point of detection. This broadening overcomes the signal intensity enhancements that might arise from the concomitant shortening of the T_1 s of Cho in the ion-pair. Thus 40% of the Cho pool is accessible to the contrast agent residing in the extracellular space. A potentially complicating factor to any interpretation is the fact that the resonance detected by in vivo MRS is a composite peak, comprised of several different compounds that cannot be resolved in vivo. These include Cho, phosphocholine, and glycerophosphocholine.

The underlying mechanisms that result in elevations of the total Cho resonance in human breast cancer have been the subject of many studies (for example, see Refs. 32–35). Cho is considered an essential nutrient in mammals, and the major source of Cho is from the diet (36,37). Normally, the concentration of Cho in human plasma is in the range

of 5–10 μ M (38,39). Specific active transporters facilitate the uptake of Cho into cells (40,41), where it is metabolized through the Kennedy pathway (see Fig. 1 in Ref. 33). The first step in this pathway is the phosphorylation of Cho by the enzyme choline kinase (ChoK). This is followed by PCho conversion to cytidyldiphosphate-choline (CDP-choline) by cytidine triphosphate (CTP):PCho cytidylyltransferase (CCT) and condensation with diacylglycerol to form phosphatidylcholine (PtdCho), which is the major phospholipid constituent of cellular membranes. Free Cho can also be regenerated by the controlled breakdown of Cho phospholipids through the activity of phospholipases D (PLDs), which produce Cho and phosphatidic acid, or through that of phospholipases A (PLAs), which generate lysoPtdCho, which is further hydrolyzed to free fatty acids and GPCCho (42). Based on all of these pathways and NMR data collected from model studies carried out in tissue culture, most investigators would conclude that the levels of extracellular Cho would be low.

Recently Sitter et al. (43,44) have published high-resolution magic angle spinning (HR MAS) spectra acquired from human breast cancer tissue. Using HR MAS, it is possible to resolve the total Cho peak into its individual components, and thus estimate the relative contribution of each of the components to the total Cho peak. In their first work, in which there were HR MAS spectra shown from six patients, we estimate that the free Cho peak represents at least 30% of the total Cho-containing compounds present (44). In their subsequent study, spectra were collected from 85 tissue specimens (43) in which the metabolite levels were averaged across groups; the percentage of Cho ranged from about 20% to 35% of the total Cho pool. Based on these data, it is possible that the extracellular level of Cho could reach levels that are high enough to account for the signal loss observed in our animal studies. Because our tumors were relatively large and appear to have a necrotic core, it is also possible that in this core there is extensive cellular breakdown resulting in the formation of compartments that contain Cho at high concentration. This Cho can come into contact with the negatively-charged gadolinium-based contrast agents.

Whatever the explanation for the decrease in the levels of Cho in the tumors that we observed, it is clear that the use of negatively-charged chelates may lead to an underestimation of the levels of Cho present in human breast cancers, since most studies use MRS postcontrast administration. Therefore, we recommend that it is more prudent, at least for the short term, to employ the neutral chelates in MRI/MRS studies of the breast. We are currently exploring the possible utility of using the negatively-charged chelates to provide an estimate of the ratio of intracellular to extracellular Cho levels in those situations where the MRS can be performed both pre- and postcontrast administration.

REFERENCES

1. Liberman L. Breast cancer screening with MRI—what are the data for patients at high risk? *N Engl J Med* 2004;351:497–500.
2. Lord SJ, Lei W, Craft P, Cawson JN, Morris I, Walleiser S, Griffiths A, Parker S, Houssami N. A systematic review of the effectiveness of magnetic resonance imaging (MRI) as an addition to mammography and ultrasound in screening young women at high risk of breast cancer. *Eur J Cancer* 2007;43:1905–1917.

3. Warner E, Messersmith H, Causer P, Eisen A, Shumak R, Plewes D. Systematic review: using magnetic resonance imaging to screen women at high risk for breast cancer. *Ann Intern Med* 2008;148:671–679.
4. Bleicher RJ, Morrow M. MRI and breast cancer: role in detection, diagnosis, and staging. *Oncology (Williston Park)* 2007;21:1521–1528.
5. Kuhl CK. Current status of breast MR imaging. Part 2. Clinical applications. *Radiology* 2007;244:672–691.
6. Morris EA. Diagnostic breast MR imaging: current status and future directions. *Radiol Clin North Am* 2007;45:863–880.
7. Saslow D, Boetes C, Burke W, Harms S, Leach MO, Lehman CD, Morris E, Pisano E, Schnall M, Sener S, Smith RA, Warner E, Yaffe M, Andrews KS, Russell CA; American Cancer Society Breast Cancer Advisory Group. American Cancer Society guidelines for breast screening with MRI as an adjunct to mammography. *CA Cancer J Clin* 2007;57:75–89.
8. Saslow D, Boetes C, Burke W, Harms S, Leach MO, Lehman CD, Morris E, Pisano E, Schnall M, Sener S, Smith RA, Warner E, Yaffe M, Andrews KS, Russell CA; American Cancer Society Breast Cancer Advisory Group. American Cancer Society guidelines for breast screening with MRI as an adjunct to mammography [Erratum]. *CA Cancer J Clin* 2007;57:185.
9. Bolan PJ, Nelson MT, Yee D, Garwood M. Imaging in breast cancer: magnetic resonance spectroscopy. *Breast Cancer Res* 2005;7:149–152.
10. Katz-Brull R, Lavin PT, Lenkinski RE. Clinical utility of proton magnetic resonance spectroscopy in characterizing breast lesions. *J Natl Cancer Inst* 2002;94:1197–1203.
11. Ronen SM, Leach MO. Imaging biochemistry: applications to breast cancer. *Breast Cancer Res* 2001;3:36–40.
12. Sharma U, Sharma R, Jagannathan NR. Characterization of breast lesions by magnetic resonance imaging (MRI) and spectroscopy (MRS). *Curr Med Imaging Rev* 2006;2:329–340.
13. Tse GM, Yeung DKY, King AD, Cheung HS, Yang WT. In vivo proton magnetic resonance spectroscopy of breast lesions: an update. *Breast Cancer Res Treat* 2007;104:249–255.
14. Joe BN, Chen VY, Salibi N, Fungtharntip P, Hildebolt CF, Bae KT. Evaluation of 1H-magnetic resonance spectroscopy of breast cancer pre- and postgadolinium administration. *Invest Radiol* 2005;40:405–411.
15. Murphy PS, Leach MO, Rowland IJ. Signal modulation in H-1 magnetic resonance spectroscopy using contrast agents: proton relaxivities of choline, creatine, and N-acetylaspartate. *Magn Reson Med* 1999;42:1155–1158.
16. Murphy PS, Leach MO, Rowland IJ. The effects of paramagnetic contrast agents on metabolite protons in aqueous solution. *Phys Med Biol* 2002;47:N53–N59.
17. Lin AP, Ross BD. Short-echo time proton MR spectroscopy in the presence of gadolinium. *J Comput Assist Tomogr* 2001;25:705–712.
18. Murphy PS, Dzik-Jurasz ASK, Leach MO, Rowland IJ. The effect of Gd-DTPA on T-1-weighted choline signal in human brain tumours. *Magn Reson Imaging* 2002;20:127–130.
19. Sijens PE, Oudkerk M, van Dijk P, Levendag PC, Vecht CJ. H-1 MR spectroscopy monitoring of changes in choline peak area and line shape after Gd-contrast administration. *Magn Reson Imaging* 1998;16:1273–1280.
20. Sijens PE, VandenBent MJ, VanDijk P, Oudkerk M. Chemical shift imaging reveals loss of brain tumor choline signal after administration of a gadolinium contrast agent. *Radiology* 1996;201:11–11.
21. Sijens PE, van den Bent MJ, Nowak PJ, van Dijk P, Oudkerk M. 1H chemical shift imaging reveals loss of brain tumor choline signal after administration of Gd-contrast. *Magn Reson Med* 1997;37:222–225.
22. Smith JK, Kwock L, Castillo M. Effects of contrast material on single-volume proton MR spectroscopy. *AJNR Am J Neuroradiol* 2000;21:1084–1089.
23. Elgavish GA, Reuben J. Aqueous lanthanide shift-reagents. 3. Interaction of ethylenediaminetetraacetate chelates with substituted ammonium cations. *J Am Chem Soc* 1977;99:1762–1765.
24. Goldberg SN, Girnan GD, Lukyanov AN, Ahmed M, Monsky WL, Gazelle GS, Huertas JC, Stuart KE, Jacobs T, Torchillin VP, Halpern EF, Kruskal JB. Percutaneous tumor ablation: increased necrosis with combined radio-frequency ablation and intravenous liposomal doxorubicin in a rat breast tumor model. *Radiology* 2002;222:797–804.
25. Bland JM, Altman DG. Statistical methods for assessing agreement between two methods of clinical measurement. *Lancet* 1986;1:307–310.
26. Bloembergen N. Proton relaxation times in paramagnetic solutions. *J Chem Phys* 1957;27:572–573.
27. Lenkinski RE, Reuben J. Line broadenings induced by lanthanide shift-reagents—concentration, frequency, and temperature effects. *J Magn Reson* 1976;21:47–56.
28. Solomon I. Relaxation processes in a system of 2 spins. *Phys Rev* 1955;99:559–565.
29. Lenkinski RE. Lanthanide complexes of peptides and proteins. In: Berliner LJ, Reuben J, editors. *Biological magnetic resonance*. New York: Plenum Press; 1984. p 23–71.
30. Caravan P, Ellison JJ, McMurry TJ, Lauffer RB. Gadolinium(III) chelates as MRI contrast agents: structure, dynamics, and applications. *Chem Rev* 1999;99:2293–2352.
31. Lenkinski RE, Reuben J. Multisite model for lanthanide shift-reagent coordination to monofunctional substrates -effects of rotational and site averaging on shifts and relaxation rates. *J Am Chem Soc* 1976;98:4065–4068.
32. Aboagye EO, Bhujwala ZM. Malignant transformation alters membrane choline phospholipid metabolism of human mammary epithelial cells. *Cancer Res* 1999;59:80–84.
33. Eliyahu G, Kreizman T, Degani H. Phosphocholine as a biomarker of breast cancer: molecular and biochemical studies. *Int J Cancer* 2007;120:1721–1730.
34. Katz-Brull R, Degani H. Kinetics of choline transport and phosphorylation in human breast cancer cells: NMR application of the zero trans method. *Anticancer Res* 1996;16:1375–1379.
35. Katz-Brull R, Seger D, Rivenson-Segal D, Rushkin E, Degani H. Metabolic markers of breast cancer: enhanced choline metabolism and reduced choline-ether-phospholipid synthesis. *Cancer Res* 2002;62:1966–1970.
36. Blusztajn JK. Developmental neuroscience: choline, a vital amine. *Science* 1998;281:794–795.
37. Zeisel SH, Dacosta KA, Franklin PD, Alexander EA, Lamont JT, Sheard NF, Beiser A. Choline, an essential nutrient for humans. *FASEB J* 1991;5:2093–2098.
38. Savendahl L, Mar MH, Underwood LE, Zeisel SH. Prolonged fasting in humans results in diminished plasma choline concentrations but does not cause liver dysfunction. *Am J Clin Nutr* 1997;66:622–625.
39. Zeisel SH, Growdon JH, Wurtman RJ, Magil SG, Logue M. Normal plasma choline responses to ingested lecithin. *Neurology* 1980;30:1226–1229.
40. Koepsell H, Endou H. The SLC22 drug transporter family. *Pflugers Arch* 2004;447:666–676.
41. Koepsell H, Schmitt BM, Gorboulev V. Organic cation transporters. *Rev Physiol Biochem Pharmacol* 2003;150:36–90.
42. Vance JE, Vance DE. Phospholipid biosynthesis in mammalian cells. *Biochem Cell Biol* 2004;82:113–128.
43. Sitter B, Lundgren S, Bathen TF, Halgunset J, Fjosne HE, Gribbestad IS. Comparison of HR MAS MR spectroscopic profiles of breast cancer tissue with clinical parameters. *NMR Biomed* 2006;19:30–40.
44. Sitter B, Sonnewald U, Spraul M, Fjosne HE, Gribbestad IS. High-resolution magic angle spinning MRS of breast cancer tissue. *NMR Biomed* 2002;15:327–337.